arXiv:0912.4479v1 [hep-ph] 22 Dec 2009

Charmonium in a hot, dense medium

David Blaschke[1,2]

[1]*Institute for Theoretical Physics, University of Wrocław, 50-204 Wrocław, Poland*
[2]*Bogoliubov Laboratory for Theoretical Physics, JINR, 141980 Dubna, Russia*

DOI: http://dx.doi.org/10.3204/DESY-PROC-2009-07/blaschke_david

In this lecture we apply a thermodynamic Green function formalism developed in the context of nonrelativistic plasma physics for the case of heavy quarkonia states in strongly correlated quark matter. Besides the traditional explanation of charmonium suppresion by Debye screening of the strong interaction, we discuss further effects of relevance when heavy quarkonia states propagate in a medium where strong correlations persist in the form of hadronic resonances. These effects may be absorbed in the definition of a plasma Hamiltonian, which was the main result of this work. This plasma Hamiltonian governs the in-medium modification of the bound state energy levels as well as the lowering of the continuum edge which leads not only to the traditional Mott effect for the dissociation of bound states in a plasma, but can also be applied for a consistent calculation of the in-medium modification of quarkonium dissociation rates.

1 Introduction

In developing a theoretical approach to heavy quarkonia as messengers of the deconfinement/ hadronization transition of a quark-gluon plasma formed in a heavy-ion collision, we should aim at a unifying description where hadrons appear as bound states (clusters) of quarks and gluons. The situation is analoguous to the problem of two-particle states in QED plasmas where a well-developed theory in the framework of the Green function technique exists. These methods have been widely developed for the case of the hydrogen plasma, where the electrons and protons as the elementary constituents can form hydrogen atoms as bound states of the attractive Coulomb interaction. The problem is tractable analytically for the isolated two-particle system, with a discrete energy spectrum of bound states and a continuous spectrum of scattering states. Higher complexes, such as molecular hydrogen can also be formed.

In a many-particle system, the problem of bound state formation needs to account for medium effects. They give contributions to a plasma Hamiltonian

$$H^{\rm pl} = H^{\rm Hartree} + H^{\rm Fock} + H^{\rm Pauli} + H^{\rm MW} + H^{\rm Debye} + H^{\rm pp} + H^{\rm vdW} + \dots , \qquad (1)$$

where the first three effects, the Hartree- and Fock energies of one-particle states and the Pauli blocking for the two-particle states, are of first order with respect to the interaction and determine the mean-field approximation. The following two terms of the plasma Hamiltonian are the Montroll-Ward term giving the dynamical screening of the interaction in the self-energy, and the dynamical screening (Debye) of the interaction between the bound particles. These contributions are related to the polarization function and are of particular interest for plasmas due to the long-range character of the Coulomb interaction. In a consistent description, both terms should be treated simultaneously. The last two contributions to the plasma Hamiltonian are of second order with respect to the fugacity: the polarization potential, describing the interaction of a bound state with free charge carriers, and the van der Waals interaction, accounting for the influence of correlations (including bound states) in the medium on the two-particle system under consideration, see [1, 2].

Approximations to medium effects in the self-energy and the effective interaction kernel have to be made in a consistent way, resulting in predictions for the modification of one-particle and two-particle states. On this basis, the kinetics of bound state formation and breakup processes can be described, establishing the ionization equilibrium under given thermodynamical conditions [3]. Coulomb systems similar to the hydrogen plasma are electron-hole plasmas in semiconductors [4], where excitons and biexitons play the role of the atoms and molecules. Other systems which have been widely studied are expanded fluids like alkali plasmas or noble gas plasmas, see [1] and references therein. Applications of the plasma physics concepts for cluster formation and Mott effect to the rather short-ranged strong interactions have been given, e.g., in [5, 6] for nuclear matter and in [7, 8] for quark matter.

In this subsection, we want to discuss basic insights from these investigations of bound state formation in plasmas, as far as they can concern our discussion of heavy quarkonia formation in hot and dense matter. Before going more into the details, let us mention them. Bound state properties remain rather inert to changes of the medium since the self-energy and interaction effects partially compensate each other in lowest order of density. Also, the smaller size of the bound states matters in this respect. The compensation does not hold for continuum states, being influenced by self-energy effects only, so that a lowering of the in-medium ionization threshold must occur which leads to a strong enhancement of the rate coefficients for bound-free transitions and to a sequential "melting" of different bound state excitation levels into the continuum of scattering states at corresponding critical plasma parameters (Mott effect [9]), until even the ground state becomes unbound.

The theory of strongly coupled plasmas has been developed also for strong nonideality, where the formation of clusters in the medium need to be taken into account. This situation is similar to that of a hadronizing quark-gluon plasma and we will therefore refer to cluster expansion techniques as the theoretical basis.

2 Bethe-Salpeter equation and plasma Hamiltonian

The most systematic approach to the description of bound states in plasmas uses the Bethe-Salpeter equation (BSE) for the thermodynamic (Matsubara-) two-particle Green function

$$G_{ab} = G^0_{ab} + G^0_{ab}\; K_{ab}\; G_{ab} = G^0_{ab} + G^0_{ab}\; T_{ab}\; G^0_{ab}\ , \tag{2}$$

which is equivalent to the use of the two-particle T-matrix T_{ab} and has to be solved in conjunction with the Dyson equation for the full one-particle Green function,

$$G_a = G^0_a + G^0_a \Sigma_a G_a\ , \tag{3}$$

defined by the dynamical self-energy $\Sigma_a(p,\omega)$ and the free one-particle Green function $G^0_a(p,\omega) = [\omega - \varepsilon_a(p)]^{-1}$ for a particle of species a with the dispersion relation $\varepsilon_a(p) = \sqrt{p^2+m_a^2} \approx m_a + p^2/(2m_a)$, see Fig. 1.

The BSE contains all information about the spectrum of two-particle bound as well as scattering states in the plasma. A proper formulation of the plasma effects on the two-particle

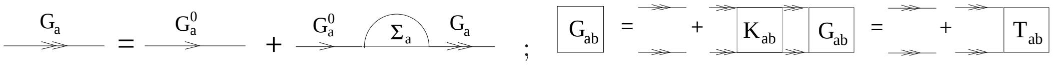

Figure 1: The two-particle problem in the medium. Dyson equation (left) and Bethe-Salpeter equation (right) need to be solved in consistent (conserving) approximations for self-energy (Σ) and interaction kernel (K).

spectrum is essential to understand why bound and scattering states are influenced in a different way by the surrounding medium, leading to the Mott-effect for bound states. We give here the essence of a detailed discussion to be found in Ref. [2].

The homogeneous BSE associated with (2) can be given the form of an effective Schrödinger equation for the wave function $\psi_{ab}(p_1, p_2, z)$ of two-particle states in the medium [4]

$$\sum_q \left\{ \left[\varepsilon_a(p_1) + \varepsilon_b(p_2) - z\right] \delta_{q,0} - V_{ab}(q) \right\} \psi_{ab}(p_1 + q, p_2 - q, z) =$$
$$= \sum_q H^{\rm pl}_{ab}(p_1, p_2, q, z) \psi_{ab}(p_1 + q, p_2 - q, z), \quad (4)$$

where a, b denote a pair of particles with 3-momenta p_1 and p_2 which transfer a 3-momentum $2q$ in their free-space interaction $V_{ab}(q)$ and z is a complex two-particle energy variable. The in-medium effects described by (2) have been singled out in the definition of a plasma Hamiltonian, containing all modifications beyond the two-body problem in free space [2, 4]

$$H^{\rm pl}_{ab}(p_1, p_2, q, z) = \underbrace{V_{ab}(q) \left[N_{ab}(p_1, p_2) - 1\right]}_{\rm (i)\ Pauli\ blocking} \underbrace{- \sum_{q'} V_{ab}(q') \left[N_{ab}(p_1 + q', p_2 - q') - 1\right] \delta_{q,0}}_{\rm (ii)\ Exchange\ self-energy}$$
$$+ \underbrace{\Delta V_{ab}(p_1, p_2, q, z) N_{ab}(p_1, p_2)}_{\rm (iii)\ Dynamically\ screened\ potential} \underbrace{- \sum_{q'} \Delta V_{ab}(p_1, p_2, q', z) N_{ab}(p_1 + q', p_2 - q') \delta_{q,0}}_{\rm (iv)\ Dynamical\ self-energy} . \quad (5)$$

Here, $\Delta V_{ab}(p_1, p_2, q, z) = K_{ab}(p_1, p_2, q, z) - V_{ab}(q)$ stands for the in-medium modification of the bare interaction potential to a dynamically screened interaction kernel $K_{ab}(p_1, p_2, q, z)$. The effects of phase space occupation are encoded in the function $N_{ab}(p_1, p_2)$, which for the case of an uncorrelated fermionic medium takes the form of the Pauli blocking factor $N_{ab}(p_1, p_2) = 1 - f_a(p_1) - f_b(p_2)$, where $f_a(p) = \{\exp[(\varepsilon_a(p) - \mu_a)/T] + 1\}^{-1}$ is the Fermi distribution and μ_a the chemical potentential of the species a. Eq. (4) is a generalization of the two-particle Schrödinger equation, where on the left-hand side the isolated two-particle problem is described while many-body effects due to the surrounding medium are given on the right-hand side. The in-medium effects named in the plasma Hamiltonian (1) can be obtained from the one derived in the Bethe-Salpeter approach (5) upon proper choice of the interaction kernel K_{ab} so that Eq. (1) appears a sa special case of Eq. (5).

The influence of the plasma Hamiltonian on the spectrum of bound and scattering states can be qualitatively discussed in perturbation theory. Since bound states are localized in coordinate space, their momentum space wave functions extend over a finite range Λ and we may assume them to be q-independent: $\psi_{ab}(p_1 + q, p_2 - q, z = E_{nP}) \approx \psi_{ab}(p_1, p_2, z = E_{nP})$ for small momentum transfer $q < \Lambda$ and to vanish otherwise. Assuming further a flat momentum dependence of the Pauli blocking factors $N_{ab}(p_1+q, p_2-q) \approx N_{ab}(p_1, p_2)$ for small q where the interaction is strong, we obtain a cancellation of the Pauli blocking term (i) by the exchange self energy (ii) and of the dynamically screened potential (iii) by the dynamical self-energy (iv). Therefore, the bound states remain largely unmodified by medium effects. For scattering states which are extended in coordinate space and can be represented by a delta function in momentum space, the above cancellations do not apply and a shift of the two-particle continuum threshold results. For this mechanism to work it is important that approximation schemes for the self-energy and the interaction kernel have to be consistent as, e.g., in the conserving scheme of Φ-derivable theories [10].

Summarizing the discussion of the plasma Hamiltonian: bound state energies remain unshifted to lowest order in the charge carrier density while the threshold for the continuum of scattering states is lowered. The intersection points of bound state energies and continuum threshold define the Mott densities (and temperatures) for bound state dissociation.

When applying this approach to heavy quarkonia in a medium where heavy quarks (either free or bound in heavy hadrons) are rare, then $N_{ab} = 1$ so that both, (i) and (ii) can be safely neglected. The effects (iii) and (iv) stem from the dynamical coupling of the two-particle state to collective excitations (plasmons) in the medium. In the screened potential approximation, the interaction kernel is represented by $V^S_{ab}(p_1p_2, q, z) = V^S_{ab}(q, z)\delta_{P,p_1+p_2}\delta_{2q,p_1-p_2}$ with

$$V^S_{ab}(q,z) = V_{ab}(q) + V_{ab}(q)\Pi_{ab}(q,z)V^S_{ab}(q,z) = V_{ab}(q)[1-\Pi_{ab}(q,z)V_{ab}(q)]^{-1} , \tag{6}$$

with the total momentum P and the momentum transfer $2q$ in the two-particle system. The most frequently used approximation for the here introduced polarization function $\Pi_{ab}(q,z)$, or for the equivalent dielectric function $\varepsilon_{ab}(q,z) = 1 - \Pi_{ab}(q,z)V_{ab}(q)$, is the random phase approximation (RPA). In the next two paragraphs we discuss the static, long wavelength limit of the RPA and its generalization for a clustered medium.

Example 1: statically screened Coulomb potential. The systematic account of the modification of the interaction potential between charged particles a and b by polarization of the medium is taken into account in the dynamical polarization function $\Pi_{ab}(q,z)$, which in RPA reads [2]

$$\Pi^{\rm RPA}_{ab}(q,z) = 2\delta_{ab}\int\frac{d^3p}{(2\pi)^3}\frac{f_a(E^a_p) - f_a(E^a_{p-q})}{E^a_p - E^a_{p-q} - z} . \tag{7}$$

For the Coulomb interaction, corresponding to the exchange of a massless vector boson, the potential is obtained from the longitudinal propagator in the Coulomb gauge is $V_{ab}(q) = e_ae_b/q^2$. For a recent discussion in the context of heavy quark correlators and potentials see, e.g., [11, 12]. Due to the large masses of the constitutents in the heavy quarkonium case, one may use a Born-Oppenheimer expansion to replace the dynamically screened interaction by its static ($z = 0$) and long-wavelength ($q \to 0$) limit. For nondegenerate systems the distribution functions are Boltzmann distributions and their difference can be expanded as

$$f_a(E^a_p) - f_a(E^a_{p-q}) = {\rm e}^{-E^a_p/T}\left(1 - {\rm e}^{-(E^a_{p-q}-E^a_p)/T}\right) \approx -f_a(E^a_p)(E^a_p - E^a_{p-q} - z)/T , \tag{8}$$

so that the energy denominator gets compensated and the polarization function becomes

$$\Pi^{\rm RPA}_{ab}(q,z) = -2\frac{\delta_{ab}}{T}\int\frac{d^3p}{(2\pi)^3}f_a(E^a_p) = -\delta_{ab}\frac{n_a(T)}{T} . \tag{9}$$

The corresponding dielectric function $\varepsilon_{ab}^{\mathrm{RPA}}(q,\omega)$ takes the form

$$\lim_{q\to 0}\varepsilon^{\mathrm{RPA}}(q,0) = 1 + \frac{\mu_D^2}{q^2}~, \quad \mu_D^2 = \frac{1}{T}\sum_a e_a^2 n_a(T)~. \tag{10}$$

The screened Coulomb potential in this approximation is therefore $V_{ab}^S(q) = V_{ab}(q)/\varepsilon^{\mathrm{RPA}}(q,0) = e_a e_b/(q^2+\mu_D^2)$. In this "classical" example of the statically screened Coulomb interaction, the contribution to the plasma Hamiltonian is real and in coordinate representation it is given by

$$\Delta V_{ab}(r) = -\frac{\alpha}{r}(\mathrm{e}^{-\mu_D r} - 1) \approx \alpha\mu_D - \frac{\alpha}{2}\mu_D^2 r~, \tag{11}$$

where $\alpha = e^2/(4\pi)$ is the fine structure constant. For the change in the Hartree self-energy of one-particle states due to Debye screening we can perform an estimate in momentum space

$$\Sigma_a = \frac{4\pi\alpha}{(2s_a+1)}\int\frac{d^3q}{(2\pi)^3}\left[\frac{1}{q^2+\mu_D^2} - \frac{1}{q^2}\right] f_a(E_q^a) \approx -\frac{\alpha\mu_D^2}{\pi}\int_0^\infty \frac{dq}{q^2+\mu_D^2} = -\frac{\alpha\mu_D}{2}~. \tag{12}$$

This entails that to lowest order in the density the shift of the one-particle energies (continuum edge of unbound states) $\Sigma_a + \Sigma_b = -\alpha\mu_D$ compensates the contribution due to the screening of the interaction (11)

$$\Delta_{ab} \approx \alpha\mu_D = \mathcal{O}(\sqrt{n a_{\mathrm{B},0}^3})~, \tag{13}$$

in the wave equation (4). For the shift of the bound state energy levels follows [2, 13]

$$\Delta E_{\mathrm{nl}} \approx -\frac{\alpha}{2}\mu_D^2\langle r\rangle_{\mathrm{nl}} = \mathcal{O}(n a_{\mathrm{B},0}^3)~, \tag{14}$$

where $a_{\mathrm{B},0} = 1/(\alpha~m)$ is the Bohr radius.

The Debye mass μ_D, equivalent to the inverse of the Debye radius r_{D} characterizing the effective range of the interaction, depends on the square root of the density $n(T)$ of charge carriers. It is this different response of bound states and scattering continuum to an increase of density and temperature in the medium which leads to the Mott effect (see, e.g., Refs. in [9] and [1]) for electrons in an insulator: bound states of the Debye potential can only exist when the Debye radius is larger than $r_{\mathrm{D,Mott}} = 0.84~a_{\mathrm{B},0}$ [14]. This entails that above a certain density even the ground state electrons become unbound and form a conduction band, resulting in an insulator-metal transition also called Mott-transition. Further details concerning this example can be found in Ref. [15].

In complete analogy to this electronic Mott effect it is expected that in hadronic matter under compression the hadrons as bound states of quarks undergo a Mott transition which results in a phase transition from the color insulating phase of hadronic matter to a color conducting or even color superconducting phase of deconfined quark matter. This applies to light hadrons as well as to heavy quarkonia, whereby due to the different scales of Bohr radii the Mott dissociation of heavy quarkonia occurs at higher densities than for light hadrons.

In most approaches the quark self energy effects are neglected and one is left with the only medium effect due to a statically screened potential. This has the consequence that in such a picture the continuum edge of the scattering states remains unshifted and due to the lack of compensation the effective interaction leads to a strong medium dependence of the bound state energies (masses). For the electron-hole plasma in highly excited semiconductors it could be shown experimentally, however, that the compensation picture is correct and the bound state energies remain almost unshifted [16].

One may of course absorb the self-energy effects into a redefinition of the effective interaction, by adding a homogeneous mean-field contribution. This is equivalent to the use of the Ecker-Weitzel potential [17]

$$V_{\mathrm{Ecker-Weitzel}}(r) = -\frac{\alpha}{r}\mathrm{e}^{-\mu_D r} - \alpha\mu_D \ . \tag{15}$$

It is interesting to note that recent investigations of the screening problem in the context of Debye-Hückel theory [18] and $Q\bar{Q}$ correlators [11, 12] have obtained this continuum shift ($-\alpha\mu_D$) as a homogeneous background field contribution. According to the above lesson from plasma physics, however, this contribution should be attributed to the self-energy of the constituents rather than to the interaction kernel, since it determines the shift of the continuum edge.

For the development of a comprehensive approach to heavy quarkonia in hadronizing hot, dense QCD matter another insight from plasma physics may be of relevance and will be discussed next: the effect of strong correlations (bound states) in the medium. To this end, the bound states will be treated like a new species occuring in the system. Accordingly, additional diagrams have to be taken into account which stem from a cluster expansion of the interaction kernel K_{ab} and the corresponding self-energy Σ_a, see Figs. 2-4. This leads in the plasma Hamiltonian H^{pl} to a generalization of the self-energy contributions (cluster-Hartree-Fock approximation), the distribution functions in the Pauli-blocking factors and the dynamical screening (cluster-RPA). The van-der-Waals interaction in Eq. (1) appears naturally as a contribution in the cluster expansion, describing polarization effects due to bound states in the medium.

3 Cluster expansion for quarkonia in correlated medium

In the vicinity of the plasma phase transition, correlations play an important role and their proper accounting requires rather sophisticated theoretical methods such as cluster expansion techniques. For the problem of charmonium in dense hadronic matter at the deconfinement transition, i.e. in the strong coupling case, we suggest a systematic Born series expansion of collisions with free and bound states in the surrounding matter so that all terms linear in the density of free particles and bound states are taken into account.

We describe the cluster expansion here in terms of its diagrammatic expressions for the interaction kernel and the corresponding self-energy. The 1^{st} Born approximation diagrams of this expansion are given in Fig. 2, see also the monograph [2]. The wavy line denotes the dynamically screened interaction V^S_{ab}, which in a strongly correlated plasma receives contributions from the polarization of the medium beyond the RPA, denoted as generalized (cluster-) RPA in Fig. 4, see Ref. [19]. Bound and scattering states are described consistently in the two-particle T-matrices. For a generalization to higher n-particle correlations, see [6, 20] and the monograph [2]. The diagrams containing T-matrices do not contribute to the charmonium spectrum as long as the densities of the charmed quarks and of charmed hadrons in the medium are negligible. This is the situation expected for the rather low-energy CBM experiment. For the discussion of charmonium production at RHIC and at LHC the inclusion of these terms can be invoked.

At the 2^{nd} Born order, we distinguish two classes of collisions with light clusters (hadrons)

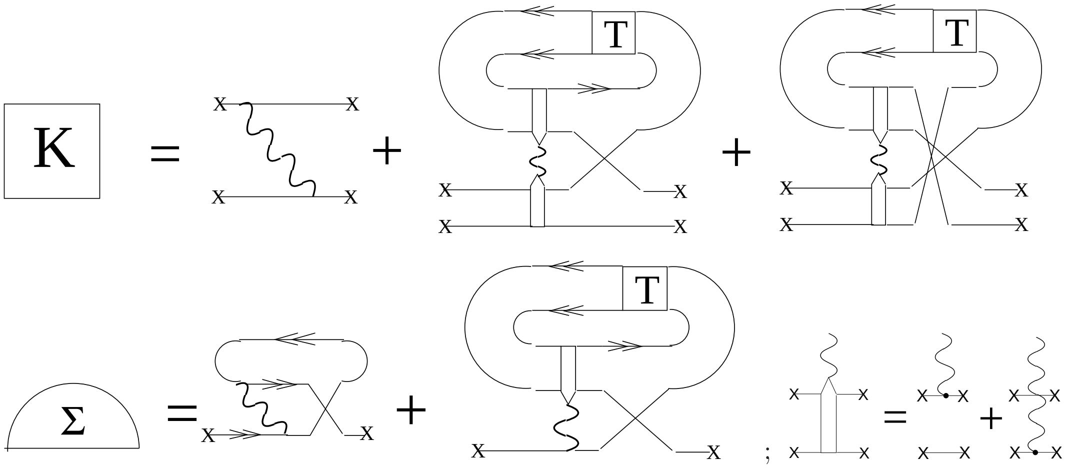

Figure 2: Cluster expansion for interaction kernel for the two-particle problem in a strongly correlated medium (upper equation) and the corresponding self-energy (lower left equation) with a dipole ansatz for the vertex (lower right equation).

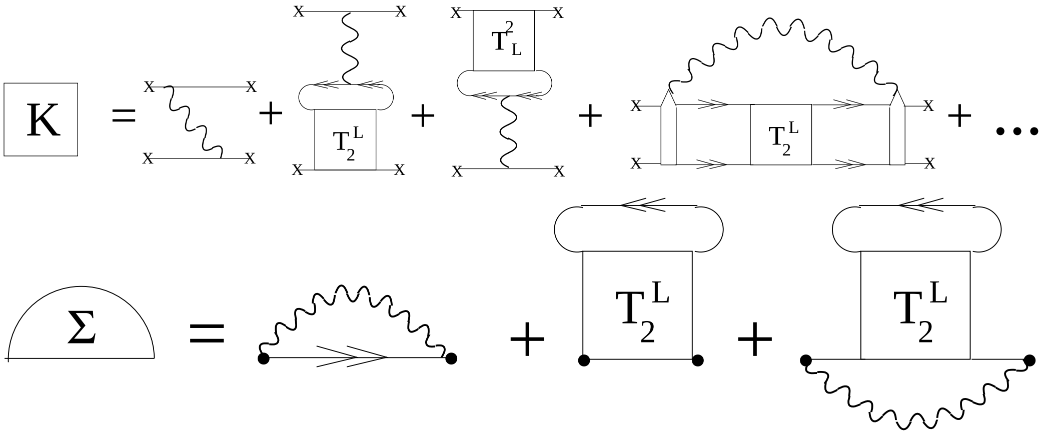

Figure 3: Alternative way of drawing the diagrams for the cluster expansion of the interaction kernel and the corresponding self-energy of Fig. 2 in a form familiar in plasma physics and nuclear physics.

that can give rise to spectral broadening of the charmonia. The first class concerns hadron impact without quark rearrangement inducing transitions to excited states, shown in the left panel of Fig. 5. These processes have been considered for charmonium-hadron interactions within the operator product expansion techniques following Peskin and Bhanot [21, 22], see [23, 24]. The result is a deformation of the charmonium spectrum under conservation of the spectral weight integrated over all charmonia states. In the second class are quark rearrangement (string-flip) processes, as indicated in the right panel of Fig. 5. They induce transitions to open charm hadrons responsible for charmonium dissociation in hadronic matter, cf. Sect. 4.

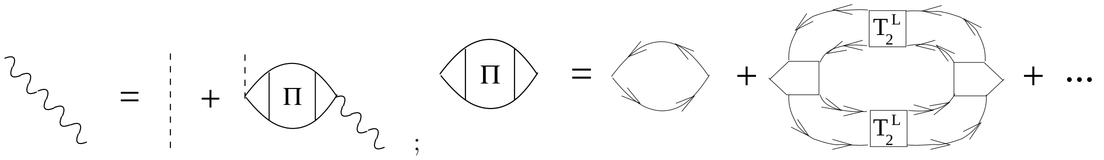

Figure 4: Left panel: The dynamically screened interaction potential $V^S_{ab}(\omega, q)$ (wavy line), determined by the bare potential (dashed line) and the polarization function $\Pi_{ab}(\omega, q)$. Right panel: Cluster expansion for the generalized RPA, when besides free particles (RPA) also two-particle states (cluster-RPA) contribute to the polarizability of the medium, see Ref. [19].

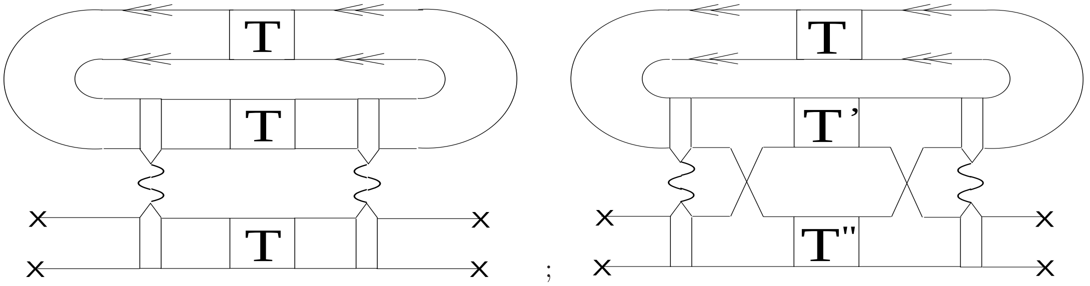

Figure 5: Contributions to the dynamical self-energy of a two-particle system in a correlated medium at 2^{nd} Born order. Left panel: impact by two-particle states without constituent exchange (van-der-Waals or dipole-dipole interaction). Right panel: constituent-rearrangement collisions (string-flip process), from Ref. [25], see also [26].

Example 2: String-flip model of charmonium dissociation. Here we give a second example for the use of insights from plasma physics by discussing charmonium dissociation within the string-flip model of quark matter [7, 8, 27, 28]. In this model the string-type color interactions between quarks get saturated within the sphere of nearest neighbors so that in a dense system of overlapping quark-antiquark pairs frequent string-flip processes take place in order to assure the system is at any time in its minimal energy configuration, see the left panel of Fig. 6.

When considering a heavy quark-antiquark pair in dense matter with negligible heavy-flavor fraction, the Pauli blocking and exchange self-energy contributions are negligible, but the strong correlations with light quarks of complementary color within the nearest neighbor sphere will result in a meanfield selfenergy shift (Hartree shift Δ^H) for all quarks [29]. This determines the shift of the continuum edge, see the graph (b) in the right panel of Fig. 6. Because of the compensation in the Bethe-Salpeter kernel between the effects of the screening of the interaction and the self energy shifts calculated with it (see discussion above), it is suggested that to lowest order the bound state energies remain unshifted when increasing the temperature and/or density of the medium. In contrast to the first example of Debye screening of long-range Coulombic interactions, the screening mechanism in the string flip model is color saturation within nearest neighbors, applicable for strong, short-range interactions as appropriate for the case of the sQGP at RHIC or dense systems at FAIR CBM. The resulting two-particle energy spectrum for charmonium and bottomonium states is shown in the right panel of Fig. 6, where the static screening picture (graph (a) as a function of the screening parameter $\mu = \mu_D(T)$ in the

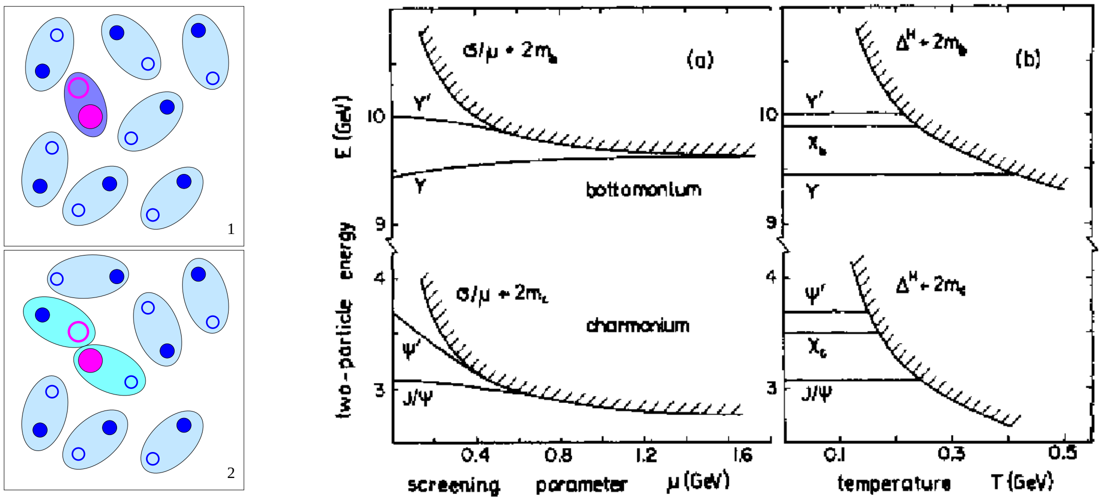

Figure 6: Left panel: String-flip process in a dense quark-antiquark system, see also [8, 26]. Right panel: Two-particle energies of charmonia and bottomonia states in a statically screened potential (a) and in the string-flip model (b), from Ref. [31].

screened Cornell potential [30] is compared to the string-flip picture (graph (b) as a function of the temperature T), from Ref. [29, 31]. From this Figure one can read-off the in-medium lowering of the dissociation threshold $k_0^{\rm diss}$, which is the energy difference between the considered bound state level and the continuum edge shown as the border of the hatched region. This lowering of $k_0^{\rm diss}$ with increasing density and/or temperature leads to a strong increase in the quarkonium breakup cross sections by thermal impact [31] and to the bound state dissociation, even before the binding energies vanish at the critical Mott densities and temperatures for the corresponding states.

4 Charmonium dissociation in a resonance gas

An interesting phenomenological guideline for the present discussion is provided by Ref. [32] where the authors show that universal J/ψ-hadron breakup cross sections with correct kinematic thresholds but otherwise constant at 3 mb for meson and 5 mb for baryon impact are sufficient to explain the observed anomalous J/ψ suppression pattern of the NA50 experiment within a multi-component hadron gas. For a recent update, see [33]. The question arises: How do these assumptions relate to microscopic calculations of charmonium dissociation reactions in hadronic matter? Those can generally be divided into two categories, based on hadronic or quark degrees of freedom. We will primarily review and compare the studies of processes in a mesonic medium (predominantly composed of pions and rho mesons) within both approaches, including a discussion of in-medium effects.

Historically, a first calculation of the quark-exchange reaction, $J/\psi + \pi \to D + \bar{D}^* + c.c.$, was performed in a nonrelativistic quark model [34] based on applications of the diagrammatic technique developed by Barnes and Swanson [35] for meson-meson scattering, see also Ref. [36]. This calculation showed a strong energy dependence of the cross section with a peak value

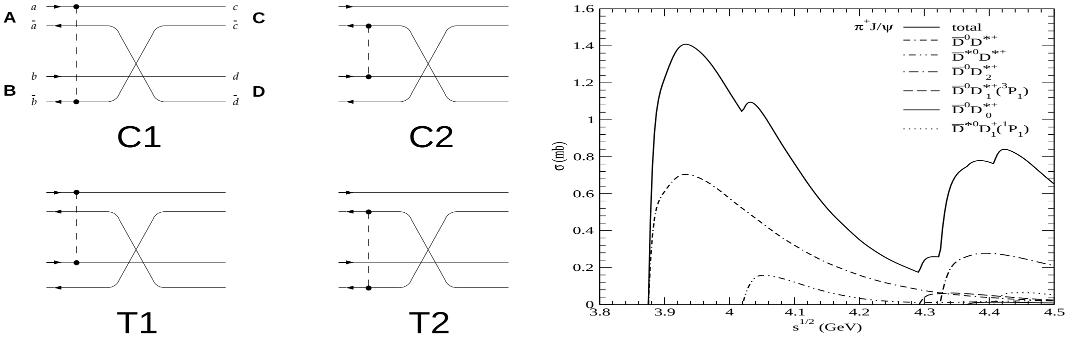

Figure 7: Born diagrams for quark-exchange processes (denoted as C1, C2 for "capture" and T1, T2 for "transfer" diagrams) contributing to heavy quarkonium dissociation by meson impact (left panels) and the corresponding cross section for J/ψ breakup by pion impact (right panel); from Refs. [37, 38]. Note that in the total cross section also the processes with charge conjugated final states are accounted for.

of about 6 mb at threshold and a fast decrease due to a momentum mismatch in the overlap integrals between the meson wave functions. The thermally averaged cross section, which is the relevant quantity for estimating the J/ψ dissociation rate, was below 1 mb, roughly in accordance with phenomenological expectations based on the observed suppression in heavy-ion reactions at the SPS. These calculations were extended to other light mesons and excited charmonia in Refs. [37, 38], where also more realistic quark-interaction potentials have been used. In Fig. 7 we show the diagrams for quark-exchange processes at first Born order, which are classified as "capture" (C) and "transfer" (T) diagrams depending on whether the quark interaction can be absorbed into the external meson lines; the latter are to be understood as a resummation of ladder-type quark-antiquark interactions. There are cancellations among the contributions of the different diagrams due to the small color dipole of the charmonium state. These cancellations reduce the peak value of the cross section to about 1 mb, as also illustrated in Fig. 7. An open question in this approach is whether the double nature of the pion – a Goldstone boson of the broken chiral symmetry and a strongly bound quark-antiquark – has a strong influence on these results. In the nonrelativistic approach the pion emerges due to a large hyperfine splitting in the Fermi-Breit Hamiltonian (as opposed to, e.g., instanton-induced interactions), which is not a robust interpretation. Another question concerns the applicability of the truncation of the transfer diagram contributions at the first Born order. Ladder-type resummations would lead to s- and t-channel D-meson exchange processes, which are disregarded in the nonrelativistic quark exchange. Finally, these models are beset with the "post-prior" problem due to the ambiguity in the ordering of quark exchange and interaction lines.

These problems can be resolved within relativistic quark models developed on the basis of Dyson-Schwinger equations [39] for applications to the charmonium dissociation problem [40, 41, 42]. In this approach, the meson-meson interactions are represented by quark-loop diagrams with three (triangle) and four (box) meson legs. The appearance of meson-exchange processes can be understood as a ladder resummation of quark interaction diagrams in s- and t-channels, see Fig. 8. The results for the J/ψ dissociation cross section by pion impact within the relativistic quark model [41], shown in Fig. 8, basically confirm those of the nonrelativistic

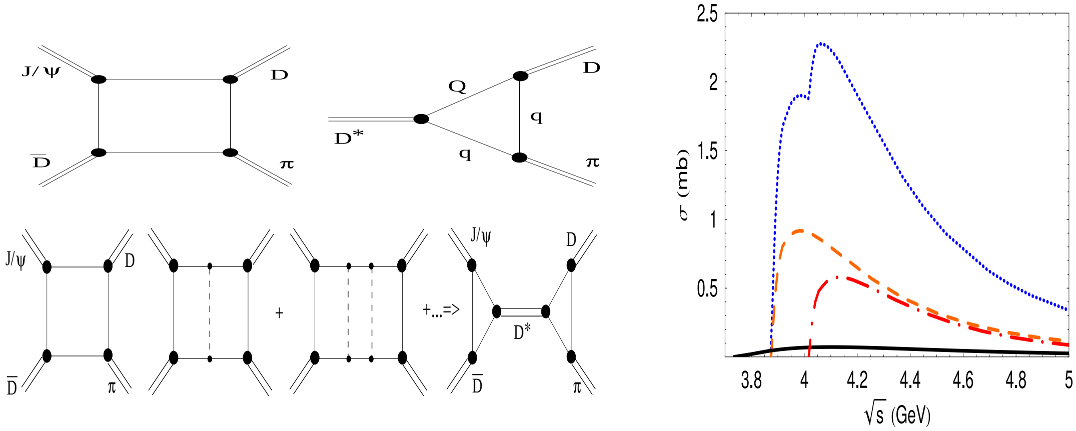

Figure 8: Left panel: box and triangle diagrams for meson-meson interaction vertices contributing to J/ψ breakup by meson impact in the relativistic quark model [40] (upper part), and the origin of D-meson exchange from ladder-type resummation (lower part). Right panel: cross section for pion induced J/ψ dissociation into open-charm mesons (dotted line) composed of subprocesses with different final-state D-meson pairs: $D+\bar{D}$ (solid), $D+\bar{D}^*$ (dashed), $D^*+\bar{D}^*$ (dash-dotted); from Ref. [41]. The total cross section includes also the subprocess with $\bar{D}+D^*$ final state for which the cross section is identical to the charge conjugated one (dashed).

approaches [34, 37, 38] shown in Fig. 7; residual differences may be traced back to the treatment of the transfer-type diagrams. In the relativistic treatment these diagrams are resummed beyond the first Born approximation and result in D-meson exchange diagrams which are absent in the nonrelativistic models. This difference may explain small differences in cross section results from both approaches.

Already in 1998, Matinyan and Müller [43] pioneered an alternative approach to charmonium absorption by light mesons on the basis of an effective meson Lagrangian, with a local $U(4)$ flavor symmetry strongly broken by the pseudoscalar and vector meson mass matrices. This initial version of the chiral Lagrangian approach gave rather small cross sections, $\sigma_{\pi\psi} \approx 0.3$ mb at threshold. It turned out [44, 45] that triple vector-meson couplings and contact terms, not included in Ref. [43], result in an increase of the breakup cross section by up two orders of magnitude, with a rising energy dependence. A problem for the chiral Lagrangian approaches is the treatment of hadrons as pointlike objects, which, as usual for an effective theory, becomes unreliable at high momentum transfers (due to quark-exchange substructure effects). The composite nature of hadrons can be accounted for in an approximate way by vertex form factors [45, 46], which reduce the magnitude, and affect the energy dependence, of the cross sections, see Fig. 9. The choice of the cutoff parameters in the form factors has a large effect on the charmonium breakup cross sections and remains a matter of debate [48, 49, 50, 51]. Progress may be made by calibrating the form factors with microscopic approaches as, e.g., the nonrelativistic or the relativistic quark models [52]. While the calculations with the relativistic quark model are very cumbersome, the chiral Lagrangian models offer a very effective tool to assess many other dissociation processes required for phenomenology, once the formfactor question is settled. In particular, these applications include dissociation processes by nucleon

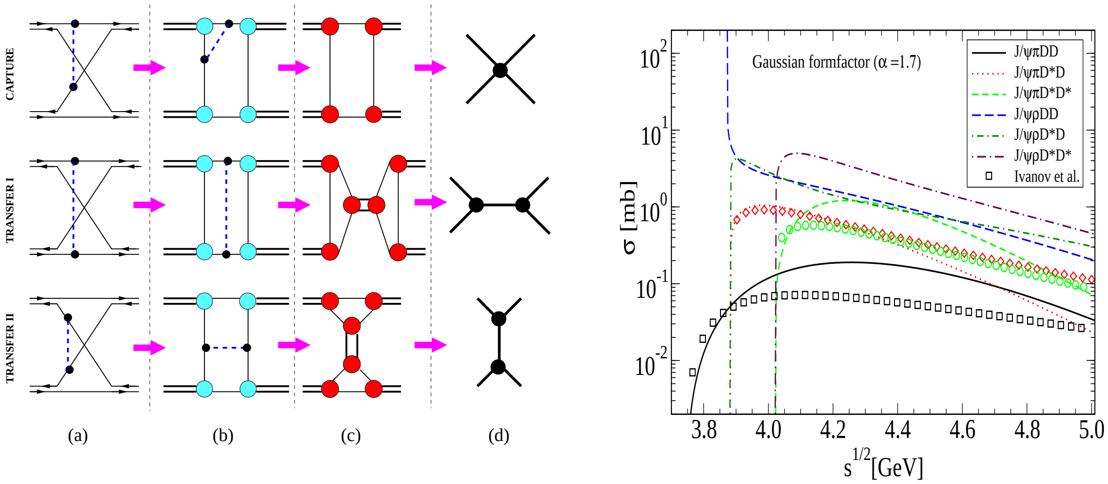

Figure 9: Feynman diagrams for J/ψ breakup by meson impact in the chiral Lagrangian approach (left) and the resulting cross sections for pion- and rho-meson induced processes (right), from Ref. [52]. The left panel illustrates the interrelation of the different approaches to charmonium breakup cross sections: The nonrelativistic potential model diagrams (a) can be redrawn as quark loop diagrams with Born order insertions (b). The latter can be either absorbed into the nonperturbative meson-quark-antiquark vertices (c, upper line) or after partial resummation of all ladder-type diagrams of the Born series redrawn as t-channel and s-channel meson exchanges (c, lower lines). The locan limit of the relativistic quark model diagrams (c) leads to the chiral Lagrangian diagrams (d) with formfactors originating from the quark loop diagrams for the meson vertices in (c).

impact [53, 54] and bottomonium dissociation [55].

The energy dependent cross sections for heavy quarkonia dissociation by hadron impact enable to evaluate the temperature- (and density-) dependent dissociation rates in hadronic matter. Assuming the (short-distance) vertex functions not to be altered by the surrounding medium, there remains the issue of mass and widths changes of open-charm hadrons with temperature and density. These, in particular, imply modifications of the thresholds for the breakup processes [58, 59, 60, 61, 62, 63]. In Fig. 10 we show the diagrammatic representation of the quark-exchange contribution to the J/ψ self-energy which develops an imaginary part (determining its width or inverse lifetime) due to the coupling to open-charm mesons. For the interaction vertex $U_{\rm ex}$ three different approaches have been discussed above and the corresponding vacuum cross sections are shown in Figs. 7-9. The theoretical basis for the discussion of quark exchange effects to the self-energy of heavy quarkonia in strongly correlated quark matter comes from systematic cluster expansion techniques developed in the context of plasma physics. For details, see the next subsection and Figs. 2, 3 and 5. Fig. 11 illustrates the effect of the spectral broadening of D-mesons at the chiral phase transition due to the opening of the decay channel into their quark constituents (Mott effect) for temperatures exceeding the D-meson Mott temperature $T^{\rm Mott} \approx 172$ MeV. Due to an effective lowering of the J/ψ breakup

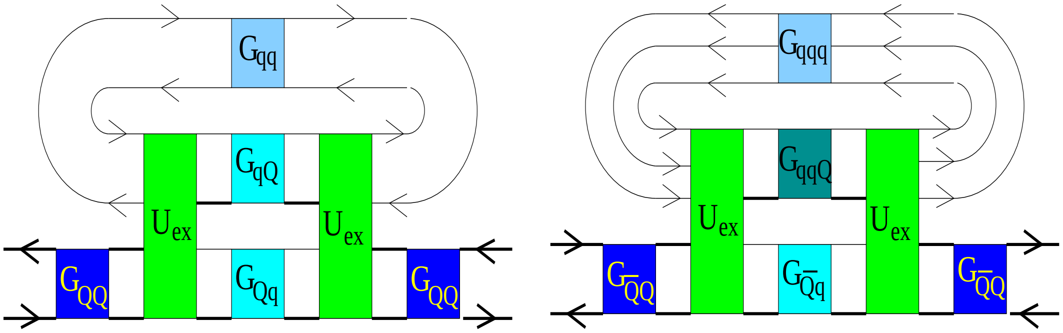

Figure 10: Left panel: Diagrammatic representation of the quark exchange process contribution to the heavy quarkonium self-energy in a mesonic medium [64]; right panel: same as left panel but for quark exchange with baryons in the medium [57]. Three different approaches to the interaction vertex $U_{\rm ex}$ are discussed in the text and shown in Figs. 7-9. Diagrams of this type appear in the cluster expansion for two-particle properties, see Fig. 5.

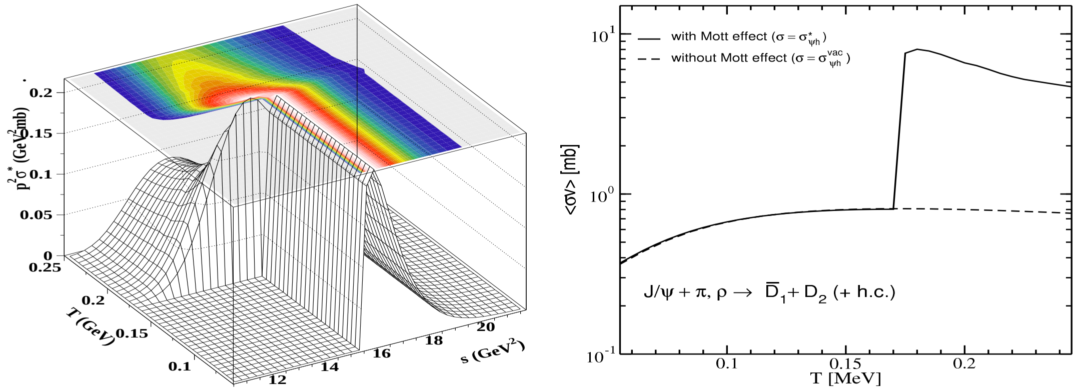

Figure 11: Left panel: energy (s) and temperature (T) dependence of the effective cross section (σ^*) for J/ψ breakup by ρ-meson impact. We display $p^2\sigma^*(s;T)$ for better visibility of the effective lowering of the breakup threshold when temperatures exceed the D-meson Mott temperature $T^{\rm Mott} \approx 172$ MeV; right panel: temperature dependence of the thermally averaged J/ψ breakup cross section in a π-ρ meson gas; the calculation with vacuum D-mesons (dashed line) is compared to one with an in-medium broadening of the D-meson spectral function (due to the Mott effect at the chiral phase transition) which exhibits a steplike enhancement (solid line) caused by the effective lowering of the breakup threshold; from Ref. [56].

threshold the temperature dependence of the thermally averaged J/ψ breakup cross section in a π-ρ meson gas exhibits a steplike enhancement [56]. This effect has been discussed as a possible mechanism underlying the threshold-like anomalous suppression pattern of J/ψ's observed by the CERN NA50 experiment [61, 64] and should also play a role in explaining the final state interactions of heavy quarkonia produced in the RHIC experiments.

5 Perspectives

In this lecture we have adapted a general thermodynamic Green function formalism developed in the context of nonrelativistic plasma physics for the case of heavy quarkonia states in strongly correlated quark matter. Besides the traditional folklore explanation of charmonium suppresion by (Debye-) screening of the strong interaction, we discuss further effects of relevance when heavy quarkonia states propagate in a medium where strong correlations persist in the form of hadronic resonances. These effects may be absorbed in the definition of a plasma Hamiltonian, which was the main result of this contribution. This plasma Hamiltonian governs the in-medium modification of the bound state energy levels as well as the lowering of the continuum edge which leads not only to the traditional Mott effect for the dissociation of bound states in a plasma, but can also be applied to calculate the in-medium modification of quarkonium dissociation rates in a consistent way. A detailed recent review [65] summarizes the phenomenological applications to heavy quarkonia production heavy-ion collision experiments at CERN and RHIC. Further developments of the presented approach shall include in particular applications to quarkonia production in dense baryonic matter such as envisaged for the PANDA and CBM experiments at FAIR Darmstadt and possibly also for NICA at JINR Dubna.

Acknowledgments

This work has been supported in part by the Polish Ministry for Science and Higher Education (MNiSW) under grants No. N N 202 0953 33 and No. N N 202 2318 37, and by the Russian Fund for Fundamental Investigations (RFFI) under grant No. 08-02-01003-a.

References

[1] R. Redmer, Phys. Rep. **282** (1997) 35.

[2] W. Ebeling, W.-D. Kraeft, D. Kremp, G. Röpke, *Quantum Statistics of Charged Many-Particle Systems*, Plenum, New York (1986).

[3] M. Schlanges, Th. Bornath and D. Kremp, Phys. Rev. A **38** (1988) 2174.

[4] R. Zimmermann, K. Kilimann, W. D. Kraeft, D. Kremp and G. Röpke, Phys. Stat. Sol. (b) **90** (1978) 175.

[5] G. Röpke, et al., Nucl. Phys. A **379** (1982) 536.

[6] G. Röpke, et al., Nucl. Phys. A **399** (1983) 587.

[7] C. J. Horowitz, E. J. Moniz and J. W. Negele, Phys. Rev. D **31** (1985) 1689.

[8] G. Röpke, D. Blaschke and H. Schulz, Phys. Rev. D **34** (1986) 3499.

[9] N. F. Mott, Rev. Mod. Phys. **40**, 677 (1968).

[10] G. Baym, Phys. Rev. **127** (1962) 1391.

[11] N. Brambilla, J. Ghiglieri, A. Vairo and P. Petreczky, Phys. Rev. D **78** (2008) 014017.

[12] A. Beraudo, J. P. Blaizot and C. Ratti, Nucl. Phys. A **806** (2008) 312.

[13] W. Ebeling and K. Kilimann, Z. Naturforsch. **44a** (1989) 519.

[14] F. J. Rogers, H. C. Garboske Jr., and D. J. Harwood, Phys. Rev. A **1** (1970) 1577.

[15] W. D. Kraeft, D. Kremp, K. Kilimann, and H. E. DeWitt, Phys. Rev. A **42** (1990) 2340.

[16] G. W. Fehrenbach, W. Schäfer, J. Treusch, and R. G. Ulbrich, Phys. Rev. Lett. **49** (1981) 1281.

[17] G. Ecker and W. Weitzel, Ann. Phys. (Lpz.) **17** (1956) 126.

[18] V. V. Dixit, Mod. Phys. Lett. A **5** (1990) 227.

[19] G. Röpke and R. Der, Phys. stat. sol. (b) **92** (1979) 501.
[20] G. Röpke, et al., Nucl. Phys. A **424** (1984) 594.
[21] G. Bhanot and M. E. Peskin, Nucl. Phys. B **156** (1979) 391.
[22] M. E. Peskin, Nucl. Phys. B **156** (1979) 365.
[23] D. Kharzeev and H. Satz, Phys. Lett. B **334** (1994) 155.
[24] F. Arleo, P.B. Gossiaux, T. Gousset and J. Aichelin, Phys. Rev. D **65** (2002) 014005.
[25] D. Blaschke and V. L. Yudichev, AIP Conf. Proc. **842** (2006) 38.
[26] H. Satz, arXiv:hep-ph/0602245.
[27] H. Miyazawa, Phys. Rev. D **20** (1979) 2953.
[28] D. Blaschke, F. Reinholz, G. Röpke and D. Kremp, Phys. Lett. B **151** (1985) 439.
[29] G. Röpke, D. Blaschke and H. Schulz, Phys. Lett. B **202** (1988) 479.
[30] F. Karsch, M. T. Mehr and H. Satz, Z. Phys. C **37** (1988) 617.
[31] G. Röpke, D. Blaschke and H. Schulz, Phys. Rev. D **38** (1988) 3589.
[32] D. Prorok and L. Turko, Phys. Rev. C **64** (2001) 044903.
[33] D. Prorok, L. Turko and D. Blaschke, AIP Conf. Proc. **1038** (2008) 73.
[34] K. Martins, D. Blaschke and E. Quack, Phys. Rev. C **51** (1995) 2723.
[35] T. Barnes and E. S. Swanson, Phys. Rev. D **46** (1992) 131.
[36] D. Blaschke and G. Röpke, Phys. Lett. B **299** (1993) 332.
[37] C. Y. Wong, E. S. Swanson and T. Barnes, Phys. Rev. C **62** (2000) 045201.
[38] T. Barnes, E. S. Swanson, C. Y. Wong and X. M. Xu, Phys. Rev. C **68** (2003) 014903.
[39] C. D. Roberts and A. G. Williams, Prog. Part. Nucl. Phys. **33** (1994) 477.
[40] D. B. Blaschke, G. R. G. Burau, M. A. Ivanov, Yu. L. Kalinovsky and P. C. Tandy, arXiv:hep-ph/0002047.
[41] M. A. Ivanov, J. G. Körner and P. Santorelli, Phys. Rev. D **70** (2004) 014005.
[42] A. Bourque and C. Gale, Phys. Rev. C **80** (2009) 015204.
[43] S. G. Matinyan and B. Müller, Phys. Rev. C **58** (1998) 2994.
[44] K. L. Haglin, Phys. Rev. C **61** (2000) 031902.
[45] Z. W. Lin and C. M. Ko, Phys. Rev. C **62** (2000) 034903.
[46] K. L. Haglin and C. Gale, Phys. Rev. C **63** (2001) 065201.
[47] Z. W. Lin and C. M. Ko, Nucl. Phys. A **715** (2003) 533.
[48] Y. S. Oh, T. Song and S. H. Lee, Phys. Rev. C **63** (2001) 034901.
[49] V. V. Ivanov, Yu. L. Kalinovsky, D. Blaschke and G. R. G. Burau, arXiv:hep-ph/0112354.
[50] Y. S. Oh, T. S. Song, S. H. Lee and C. Y. Wong, J. Korean Phys. Soc. **43** (2003) 1003.
[51] A. Bourque, C. Gale and K. L. Haglin, Phys. Rev. C **70** (2004) 055203.
[52] D. B. Blaschke, H. Grigorian and Yu. L. Kalinovsky, arXiv:0808.1705 [hep-ph].
[53] A. Sibirtsev, K. Tsushima and A. W. Thomas, Phys. Rev. C **63** (2001) 044906.
[54] W. Liu, C. M. Ko and Z. W. Lin, Phys. Rev. C **65** (2002) 015203.
[55] Z. W. Lin and C. M. Ko, Phys. Lett. B **503** (2001) 104.
[56] D. Blaschke, G. Burau, Yu. Kalinovsky and T. Barnes, Eur. Phys. J. A **18** (2003) 547.
[57] D. Blaschke, Y. Kalinovsky and V. Yudichev, Lect. Notes Phys. **647** (2004) 366.
[58] L. Grandchamp, R. Rapp and G. E. Brown, Phys. Rev. Lett. **92** (2004) 212301.
[59] A. Sibirtsev, K. Tsushima, K. Saito and A. W. Thomas, Phys. Lett. B **484** (2000) 23.
[60] K. Tsushima, A. Sibirtsev, K. Saito, A. W. Thomas and D. H. Lu, Nucl. Phys. A **680** (2001) 280.
[61] G. R. G. Burau, D. B. Blaschke and Y. L. Kalinovsky, Phys. Lett. B **506** (2001) 297.
[62] D. Blaschke, G. Burau, Yu. Kalinovsky, V. Yudichev, Prog. Theor. Phys. Suppl. **149** (2003) 182.
[63] C. Fuchs, B. V. Martemyanov, A. Faessler and M. I. Krivoruchenko, Phys. Rev. C **73** (2006) 035204.
[64] D. Blaschke, G. Burau and Yu. L. Kalinovsky, arXiv:nucl-th/0006071.
[65] R. Rapp, D. Blaschke and P. Crochet, arXiv:0807.2470 [hep-ph].

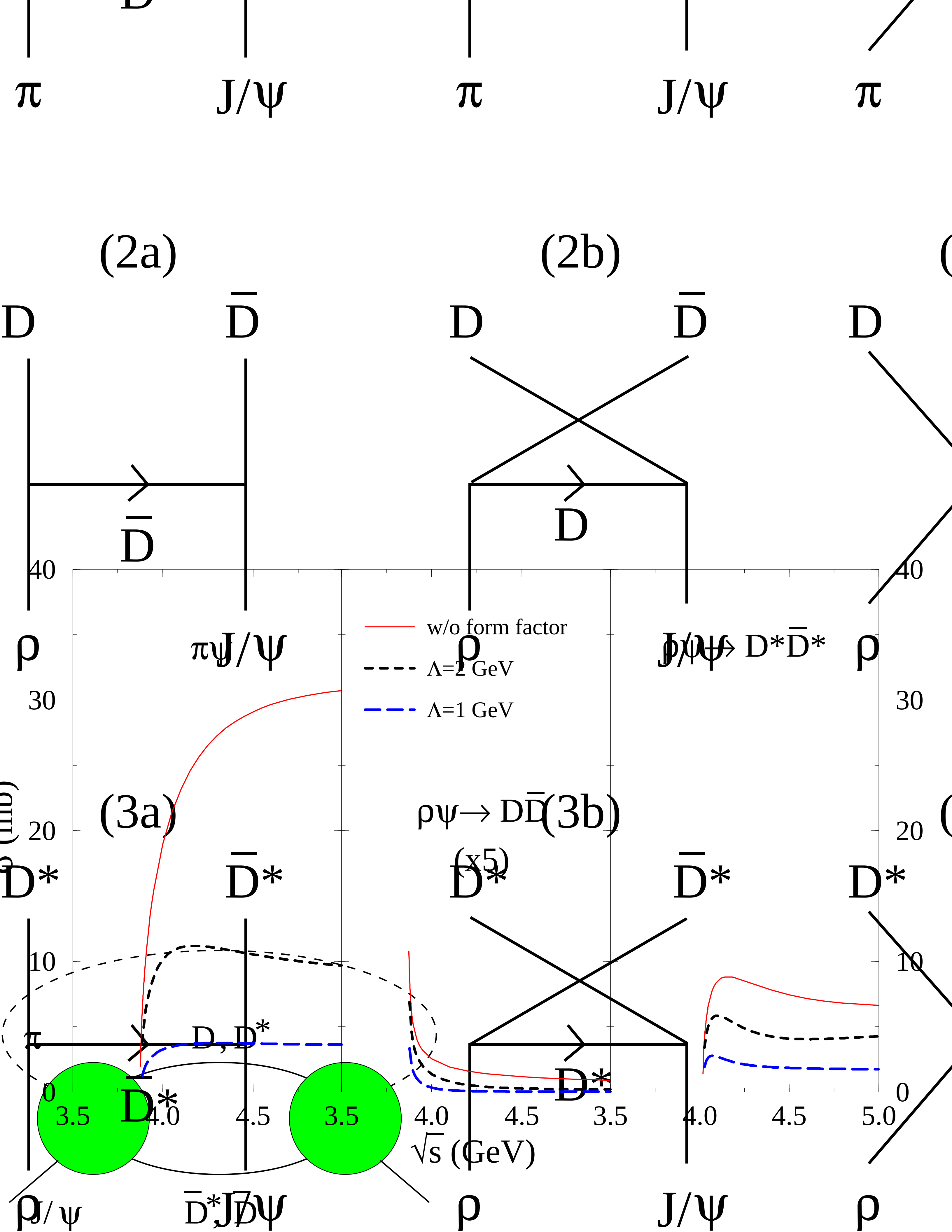
D
π
J/ψ
π
J/ψ
π
(2a)
(2b)
D
D̄
D̄
D
D̄
D
D
ρ
J/ψ
ρ
J/ψ
ρ
40
30
20
10
0
40
30
20
10
0
σ (mb)
w/o form factor
Λ=2 GeV
Λ=1 GeV
πψ
ρψ→ D*D̄*
ρψ→ DD̄
(x5)
(3a)
(3b)
D*
D̄*
D*
D̄*
D*
π
D, D*
D*
D̄*
3.5
4.0
4.5
3.5
4.0
4.5
3.5
4.0
4.5
5.0
√s (GeV)
ρ
J/ψ
ρ
J/ψ
ρ
J/ψ
D̄*, D̄